# An LPTV Noise Cancellation Technique for a 0.9-V Filtering-by-Aliasing Receiver Front-End with >67-dB Stopband Rejection

Shi Bu<sup>1</sup>, Sameed Hameed<sup>2</sup>, and Sudhakar Pamarti<sup>1</sup>
<sup>1</sup>University of California, Los Angeles, CA 90095 USA
<sup>2</sup>Silvus Technologies, Inc., Los Angeles, CA 90024 USA

Abstract—A linear periodically time-varying (LPTV) noise cancellation technique for filtering-by-aliasing (FA) receivers is presented in this paper. Fabricated in a 28-nm CMOS process, it improves the noise figure (NF) by about 3 dB while achieving over 67-dB stopband rejection with a transition bandwidth of only four times the RF BW. A minimum in-band NF of 3.2 dB is demonstrated. With an upfront N-path filter to further enhance the linearity, the measured out-of-band IIP<sub>3</sub> is +18 dBm and the blocker 1-dB compression point is +9 dBm. Operating under a 0.9-V supply, it consumes 61-mW power at 500-MHz LO.

Keywords—Linear periodically time-varying (LPTV) circuits, noise cancellation, receiver front-end, FIR filtering, software-defined radio.

### I. INTRODUCTION

In recent years, it has been of great interest to investigate highly programmable receiver architectures that achieve low noise figure (NF) [1], high linearity [2]–[5], and sharp filtering [3]–[6] for SAW/BAW-less software-defined radio (SDR) applications. They, however, either have moderate filtering [1], [2] or suffer from high NF [2]–[6] due to lack of an upfront lownoise amplifier. Moreover, their supply voltages are generally high for improving linearity.

Among them, the filtering-by-aliasing (FA) technique realizes an equivalent sharp FIR filter by utilizing linear periodically time-varying (LPTV) circuits [Fig. 1(a)] to achieve over 70-dB stopband rejection ( $A_{\text{stop}}$ ) with narrow transition band (4× RF BW) and has demonstrated high linearity [3]. Its noise, however, is fundamentally limited by contributions from the upfront LPTV resistor. While on average, this time-varying resistor achieves a low-S<sub>11</sub> matching with the antenna, during parts of each period, it can get very large (>10× the 50- $\Omega$  antenna resistance) resulting in a high NF of >6 dB [3]. This disadvantage prohibits it from being used in more generic RF environments where low NF may be desired. On the other hand, noise cancellation (NC) has been successfully implemented in prior art for linear time-invariant (LTI) and mixer-first receivers with an NF as low as 2 dB as demonstrated in [1]. As shown in Fig. 1(b), generic NC senses the noise voltage from the input matching resistor at the RF node,  $v_x$ , with a transconductance  $(G_{\rm m})$  cell and cancels this noise by subtracting the signals at the outputs of the main and NC paths.

This paper describes the *first* application of NC principle to FA-based receivers and achieve a minimum in-band NF (NF<sub>min,IB</sub>) of 3.2 dB without noticeable degradation of FA filtering performance. In principle, noise cancellation can be

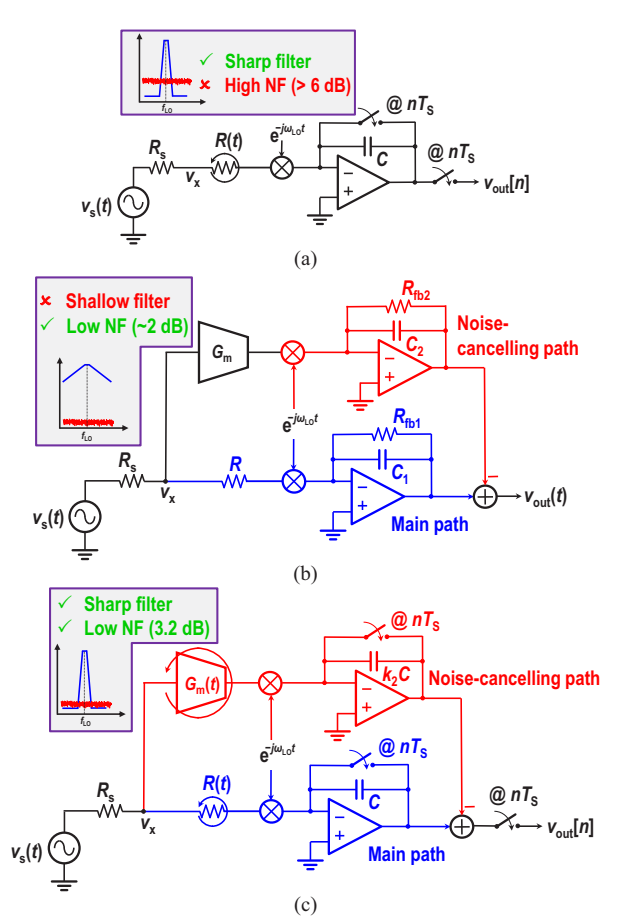


Fig. 1. (a) FA receiver using LPTV resistor for sharp filtering [3], (b) noise cancellation for mixer-first receiver using LTI  $G_m$  [1], (c) proposed LPTV noise cancellation for FA receiver with both sharp filtering and low noise

readily applied to FA-based receivers using a noise-sensing  $G_{\rm m}$  cell, *albeit* a periodically time-varying one, as shown in Fig. 1(c). However, several practical challenges need to be overcome. Foremost, proper FA operation has to be preserved such that the sharp filtering benefits of FA are retained. Secondly, the design of the NC path presents significant dynamic range and linearity challenges since the noise-sensing node,  $v_{\rm x}$ , swings much more than in conventional NC owing to the time-varying R(t).

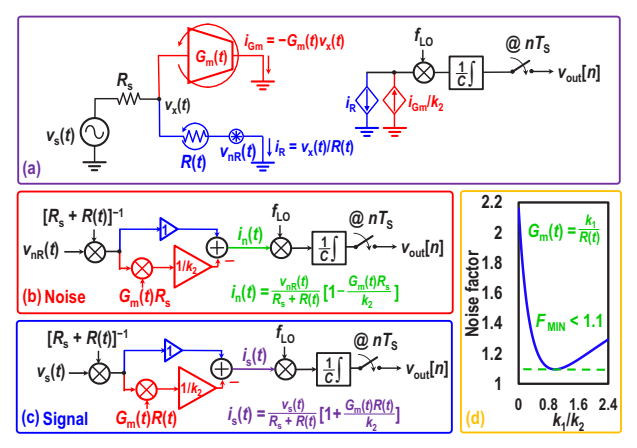


Fig. 2. Concept of the proposed technique: (a) overall equivalent model, (b) noise-path model, (c) signal-path model, and (d) simulated noise factor [omitting  $G_m(t)$ 's noise and folding noise].

The rest of this paper describes how these challenges are addressed. Measured results of the fabricated chip demonstrate an  $A_{\text{stop}}$  of 67 dB with a transition BW of 4× RF BW together with good NF while achieving an out-of-band (OOB) IIP<sub>3</sub> of +18 dBm and an OOB  $B_{1dB}$  of +9 dBm under 0.9-V supply.

# II. PROPOSED LPTV NOISE CANCELATION TECHNIQUE AND CIRCUIT IMPLEMENTATION

As mentioned before, an LPTV  $G_m(t)$  cell is used to sense

the noise of R(t),  $v_{nR}(t)$ , at node  $v_x$ , which is then down-converted, integrated, and sampled to realize the noise-canceling FA path. The equivalent signal and noise [due to R(t)] flows in the front-end are shown in Fig. 2(a):  $i_{Gm}$  and  $i_R$  are currents from the  $G_m$  cell and through R(t) flowing into their respective virtual grounds. Fig. 2(b) shows a simplified version that isolates the noise from R(t). As is evident, if  $G_m(t)$  is set to a constant  $k_2/R_s$ ,  $i_n(t) = 0$ , resulting in perfect cancellation of R(t)'s noise. However, it can be shown that the sharp FA-filter shape is not preserved at the final output and only first-order baseband (BB) filtering is seen instead.

We therefore select  $G_{\rm m}(t)=k_1/R(t)$ . Now  $i_{\rm n}(t)$  is not nulled [i.e., the noise from R(t) is not completely cancelled as  $i_{\rm n}(t)\neq 0$ ]. However, since the noise currents from the two paths, which have the same polarity, are subtracted, the overall noise after integration is still greatly cancelled (>90%). This leads to a noise factor close to one [<1.1 in simulation, Fig. 2(d)]. Furthermore, as shown in Fig. 2(c), the equivalent signal path is identical to the FA case: FA-operation is preserved, and sharp filtering achieved. Note that, just as in the LTI case, the noise of the  $G_{\rm m}$  cell is NOT cancelled.

Fig. 3 shows the block diagram of the implemented LPTV-NC receiver front-end. The values of  $k_1$  and  $k_2$  are programmable but are roughly set to 5–6 for best tradeoff between minimizing  $G_m(t)$ 's noise and area.

Although voltage gain is avoided prior to BB, as aforementioned, node  $v_x$  at the receiver RF input swings almost  $2^{\times}$  as

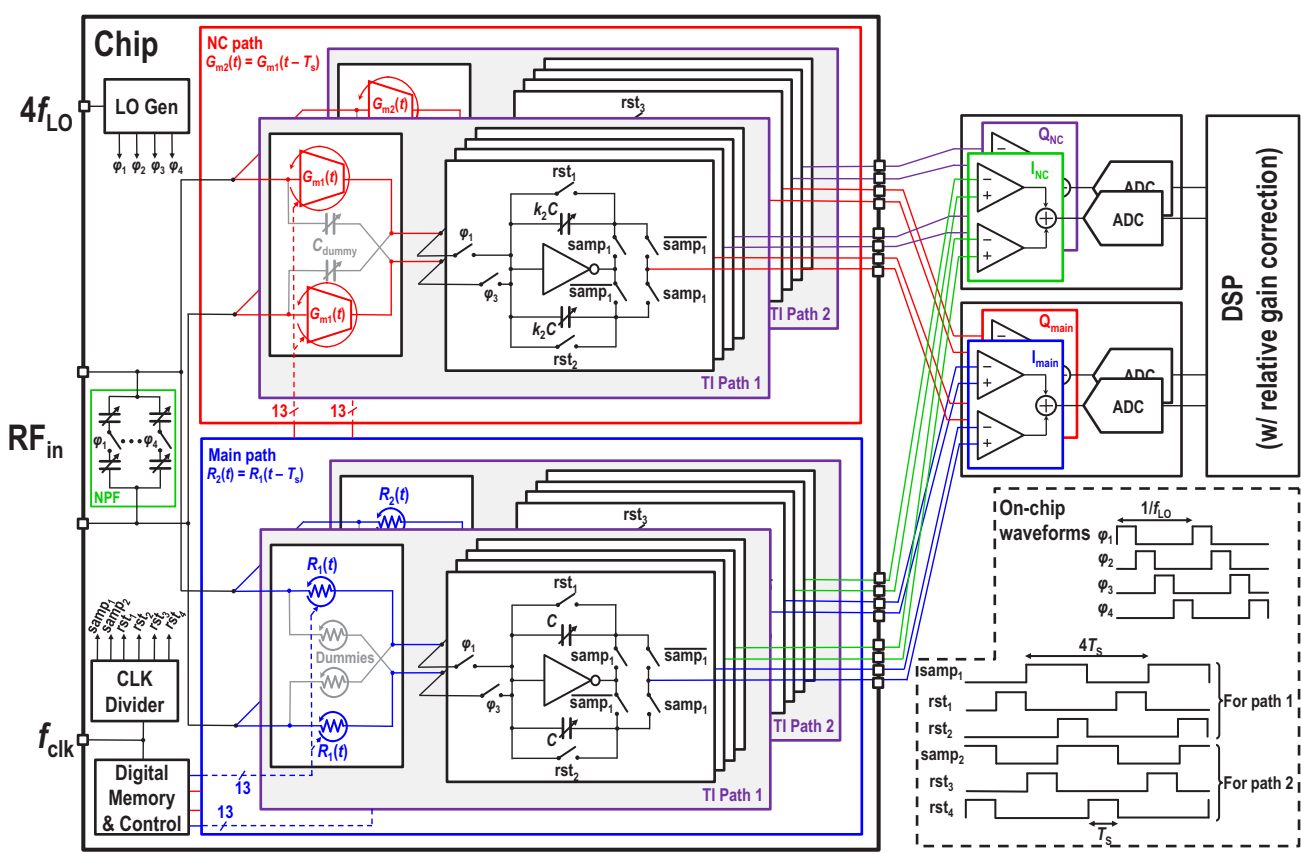


Fig. 3. Block diagram of the implemented LPTV-NC receiver front-end chip.

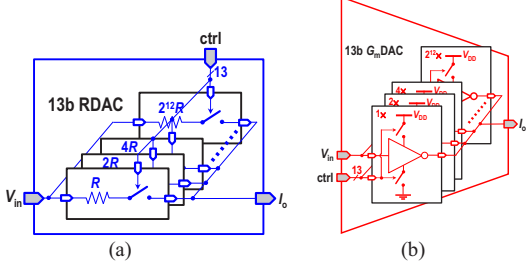


Fig. 4. Realization of (a) RDAC and (b)  $G_mDAC$ .

much as that in the simple mixer-first approach, presenting linearity challenges to the NC path which exposes the  $G_{\rm m}(t)$  block to the RF environment directly. We address this in two different ways. Firstly, time-interleaving (TI) is employed that reduces the swing of  $v_{\rm x}$  as the total input resistance is now  $R_1(t)|R_2(t)$  [3]. This also helps increase  $A_{\rm stop}$  and simplify input matching at almost no cost in NF. Both main and NC paths contain two TI paths, where one is a  $T_{\rm s}$ -delayed version of the other and  $T_{\rm s}$  is the effective sampling rate at the receiver's output. Secondly, an N-path filter (NPF) [2] is added to the RF node to further suppress the swing in the presence of OOB blockers.

 $R_{1,2}(t)$  are implemented as two 13-bit binary resistor DACs (RDACs) [Fig. 4(a)], while  $G_{m1,2}(t)$  are formed by inverterbased G<sub>m</sub> cells binarily turned ON/OFF by switches (13-bit  $G_{\rm m}$ DACs), shown in Fig. 4(b). They all vary at the rate of a clock frequency,  $f_{\text{clk}}$ , which is also used to generate all sampling and reset control clocks. The NPF is driven by the same set of 25% duty-cycle clocks at LO frequency,  $f_{LO}$ , as the 4-path passive mixer in the main and NC paths. Co-design of FA and NPF, which are both LPTV, is also nontrivial due to the fact that  $R_{1,2}(t)$ [or  $G_{m1,2}(t)$ ] and NPF do not share the same fundamental frequency and may also have different phases. While timedomain analysis works fine for each individual system, it is difficult to analyze the hybrid system in a similar manner. In this work, we work in the frequency domain and assume the NPF to be trapezoid-like with finite  $A_{\text{stop}}$ . The shape of  $R_{1,2}(t)$  [and hence  $G_{\rm ml,2}(t)$ ] is then changed accordingly to roughly maintain the same effective impulse response. This results in slightly sharper filtering while only slightly sacrificing in-band filter droop. Impedance matching requires only scaling  $R_{1,2}(t)$  after considering the in-band shunt resistance from NPF. Conversion matrices [7] were used to analyze and compute the effective hybrid LPTV filter response and impedance.

The receiver front-end consists of only switches, inverter-based amplifiers, digital circuits, plus passive devices (namely resistors and capacitors). The supply voltage,  $V_{\rm DD}$ , of the whole chip is 0.9 V. The bias of the entire chain is set to about half  $V_{\rm DD}$  by resetting BB amplifiers, and no dedicated biasing circuitry is needed. These amplifiers are sized to have 125-mS  $g_{\rm m}$  and 35-dB dc gain with ping-pong capacitor banks around them for sampling. All switches in the RDACs use minimum-length devices and the RDACs are designed to have a minimum resistance of 30  $\Omega$ . Switches in the  $G_{\rm m}$ DACs act as source-degeneration resistors to the  $G_{\rm m}$  cells and are therefore designed to contribute less than 10% of the effective  $G_{\rm m}$  for noise consideration. Non-minimum-length devices are used in the inverter-based  $G_{\rm m}$  cells for lower excessive noise factor  $\gamma$  and

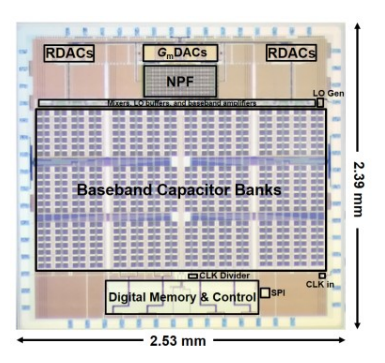


Fig. 5. Chip micrograph.

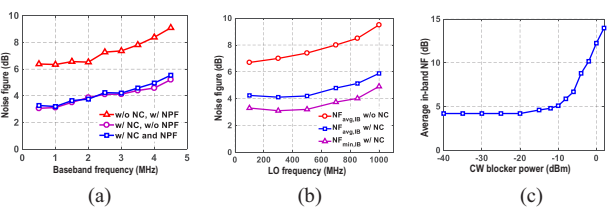


Fig. 6. (a) Measured in-band NFs with and without NC with  $f_{LO} = 500$  MHz and RF BW = 10 MHz (5-MHz baseband BW), (b) measured NF across different LO frequencies, (c) measured average in-band NF in the presence of a CW blocker at  $\Delta f = 30$  MHz with  $f_{LO} = 500$  MHz.

higher output impedance at the cost of worsened  $S_{11}$ . On average, each  $G_m DAC$  consumes 1.5-mA current. Switches in mixer and NPF are sized for ON-resistances of 2.5 and 5  $\Omega$ , respectively. BB integrator capacitors are tunable from 10 to 70 pF in the main path and 50 to 350 pF in the NC path.

### III. MEASUREMENT RESULTS

The implemented test chip was fabricated in a 28-nm CMOS process. Fig. 5 shows the die photo of the fabricated chip. The active area is  $3.75 \text{ mm}^2$ , 90% of which is BB capacitors that can be significantly reduced when designed for operation with only higher RF BWs. At  $f_{LO} = 500$  MHz, the entire chip consumes 61-mW power, in which the digital control circuitry contributes 4.7 mW at a nominal  $f_{Clk}$  of 1 GHz. The power increases with  $f_{LO}$  due to LO divider and switch drivers being more power-hungry at higher frequencies.

The outputs are buffered externally, converted to digital signals by off-chip ADCs, and then processed digitally for signal summation and subtraction. The RDACs and  $G_m$ DACs are dc calibrated at startup. Fig. 6(a) shows the measured in-band NF at 500-MHz  $f_{LO}$ . With both NPF and NC, the NF<sub>min,IB</sub> is 3.2 dB and the averaged NF over  $[0, f_s/2)$ , where  $f_s = 1/T_s$  is the output sampling frequency, NF<sub>avg,IB</sub>, is 4.2 dB. The increase of in-band NF at higher offset frequencies is due to filter droop. It is also seen that the NPF has minimal impact on the NF. Without the NPF, NF<sub>avg,IB</sub> is about 0.15-dB better. In contrast, both NF<sub>min,IB</sub> and NF<sub>avg,IB</sub> are about 3-dB worse without NC. Fig. 6(b) shows the measured NF with and without NC at different  $f_{LO}$ . The NF<sub>avg,IB</sub> is 12 dB with a 0-dBm continuous-wave (CW) blocker placed at 30-MHz offset ( $\Delta f$ ), as illustrated in Fig. 6(c), mostly limited by the phase noise of the LO divider as verified by simulation. The measured  $A_{\text{stop}}$  for the overall filter is greater than 67 dB for a transition bandwidth of 40 MHz with a gain of

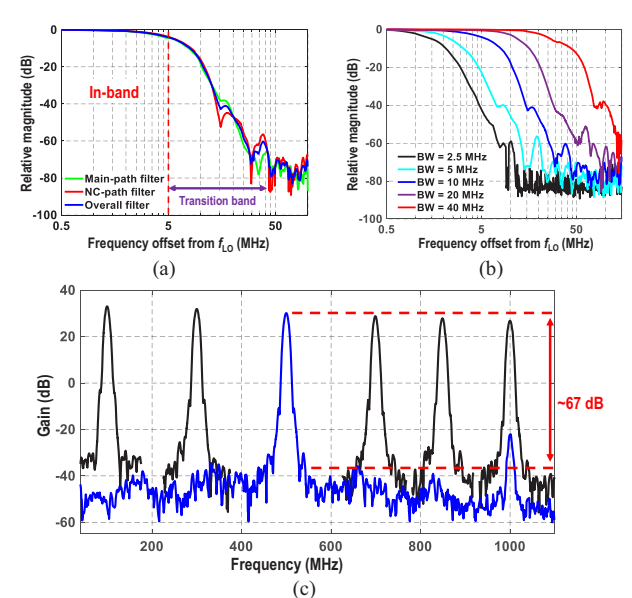


Fig. 7. (a) Measured 10-MHz RF BW filter responses, (b) filter responses with BW tuned from 2.5–40 MHz, (c) filter responses for LO frequency varied from 0.1–1 GHz.

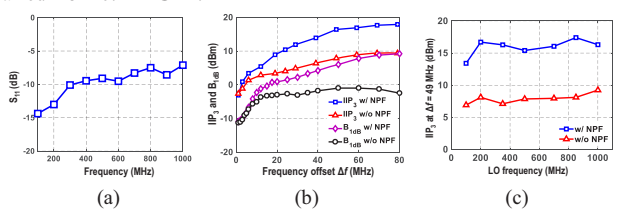


Fig. 8. (a) Measured  $S_{11}$ , (b) measured IIP<sub>3</sub> and  $B_{1dB}$  with and without NPF for  $f_{LO} = 500$  MHz, (c) measured OOB IIP<sub>3</sub> at 49-MHz offset for different LO frequencies.

~30 dB, as shown in Fig. 7(a) for 10-MHz RF BW. The achieved  $A_{\text{stop}}$  and transition bands are similar to [3] with 46- and 58-dB rejection at 22- and 30-MHz offset (using the same 67-dB  $A_{\text{stop}}$ configuration). This indicates that filter performance is preserved well with LPTV-NC. The filter can be programmed to have 5-40-MHz BW, shown in Fig. 7(b). Fig. 7(c) shows the filter responses with  $f_{LO}$  varied from 100 MHz to 1 GHz. The measured S<sub>11</sub> and linearity performance against frequency offset and  $f_{LO}$  of the receiver are depicted in Fig. 8. An OOB IIP<sub>3</sub> of +18 dBm and an OOB B<sub>1dB</sub> of +9 dBm are achieved even with upfront G<sub>m</sub>DACs thanks to the NPF. Without the NPF, both OOB B<sub>1dB</sub> and IIP<sub>3</sub> degrade evidently [Figs. 8(b) and (c)]. Table I compares this work with the state-of-the-art. While maintaining very sharp filtering with narrow transition band of FA [3], the NF compares favorably against most works. Good OOB linearity is demonstrated at a mere 0.9-V supply while other works use higher supply voltages, i.e., 1.2–1.6 V [1]–[4], [6].

## IV. CONCLUSION

In this paper, we presented an LPTV noise cancellation technique for FA-based receiver. It realizes both sharp filtering and low noise figure. The minimum in-band NF realized at 500-MHz LO is 3.2 dB, while the averaged in-band NF is 4.2 dB. The stopband rejection is 67 dB for a transition BW of 4× RF BW. OOB linearity is preserved well by inserting an NPF that helps the NC path better handle OOB blockers.

TABLE I. PERFORMANCE SUMMARY AND COMPARISON WITH THE STATE-OF-THE-ART

	[1]	[2]	[3]	[4]	[5]	This work
Arch.	FTNC	N-path	TI-FA	N-path + DT filt.	N-path	TI-FA + LPTV-NC
Tech.	40 nm	28 nm	65 nm	65 nm	65 nm	28 nm
RF freq. (GHz)	0.08–2.7	0.1–2	0.1–1	0.1–0.7	0.8–1.1	0.1–1
RF input	SE	Diff.	Diff.	Diff.	Diff.	Diff.
BW (MHz)	4	13	2.5-40	6.4-9.6	30-50	2.5-40
A <sub>stop</sub> (transition BW)	N/A	>47* (6× BW)	>45 (1.7× BW) >70 (4× BW)	>70 (8.5× BW)	>15* (0.5× BW)	>46 (1.7× BW) >67 (4× BW)
NF <sub>min,IB</sub> (dB)	1.6 @ 0.5 GHz	4.9# @ 0.5 GHz	6# @ 0.5 GHz	8.6# @ 0.5 GHz	5# @ 0.87 GHz	3.2 <sup>#</sup> @ 0.5 GHz
NF <sub>avg,IB</sub> (dB)	N/A	N/A	7# @ 0.5 GHz	N/A	~7.6*# @ 0.87 GHz	4.2 <sup>#</sup> @ 0.5 GHz
OOB IIP <sub>3</sub> (dBm)	+13.5	+44	+24	+24	+24	+18
OOB IIP <sub>2</sub> (dBm)	+55	+90	+64	N/A	N/A	+65
OOB B <sub>1dB</sub> (dBm)	-2	+13	+13	+14.7	+9	+9
Gain (dB)	72	16	23	40	-5*	30
Supply voltage (V)	1.3	1.2/1.0	1.2/1	1.2/1.6	1	0.9
Power (mW)	35–78	38–96	75–99	59–105	80–97	48–74
Area (mm²)	1.2	0.49	2.3	1.2	1.9	3.75

<sup>\*</sup> Estimated from figures

### ACKNOWLEDGMENT

The authors thank MaxLinear, Henry Chen in particular, for silicon donation and tapeout support, the National Science Foundation (grants ECCS 1408647 and ECCS 1810268) and the Broadcom Foundation for partial funding support.

# REFERENCES

- D. Murphy et al., "A blocker-tolerant, noise-cancelling receiver suitable for wideband wireless applications," *IEEE J. Solid-State Circuits*, vol. 47, no. 12, pp. 2943–2963, Dec. 2012.
- [2] Y. Lien et al., "A high-linearity CMOS receiver achieving +44dBm IIP3 and +13dBm B<sub>1dB</sub> for SAW-less LTE radio," in *IEEE Int. Solid-State Circuits Conf. (ISSCC) Dig. Tech. Papers*, San Francisco, CA, pp. 412–413, Feb. 2017.
- [3] S. Hameed and S. Pamarti, "Design and analysis of a programmable receiver front end with time-interleaved baseband analog-FIR filtering," *IEEE J. Solid-State Circuits*, vol. 53, no. 11, pp. 3197–3207, Nov. 2018.
- [4] Y. Xu and P. R. Kinget, "A switched-capacitor RF front end with embedded programmable high-order filtering," *IEEE J. Solid-State Circuits*, vol. 51, no. 5, pp. 1154–1167, May 2016.
- [5] P. Song and H. Hashemi, "A 13th-order CMOS reconfigurable RF BPF with adjustable transmission zeros for SAW-less SDR receivers," in *IEEE Int. Solid-State Circuits Conf. (ISSCC) Dig. Tech. Papers*, San Francisco, CA, pp. 416–417, Feb. 2018.
- [6] G. Qi et al., "A 0.7 to 1 GHz switched-LC N-path LNA resilient to FDD-LTE self-interference at ≥40 MHz offset," in Proc. IEEE Radio Freq. Integr. Circuits Symp. (RFIC), Honolulu, HI, pp. 276–279, May 2017.
- [7] S. Hameed et al., "Frequency-domain analysis of N-path filters using conversion matrices," *IEEE Trans. Circuits Syst. II, Exp. Briefs*, vol. 63, no. 1, pp. 74–78, Jan. 2015.

<sup>#</sup> Excludes balun loss